WATERTOWN ARSENAL LABORATORIES

DYNAMIC STRESS CONCENTRATION FACTORS

TECHNICAL REPORT WAL TR 811.6/1

BY

RICHARD SHEA

DATE OF ISSUE - MARCH 1963

AMS CODE 5011.11.838
BASIC RESEARCH IN PHYSICAL SCIENCES

D/A PROJECT 1-A-0-10501-B-010

WATERTOWN ARSENAL
WATERTOWN 72, MASS.

The findings in this report are not to be construed as an official Department of the Army position.

ASTIA AVAILABILITY NOTICE

Qualified requesters may obtain copies of this report from ASTIA

DISPOSITION INSTRUCTIONS

Destroy; do not return

AD

Dynamics (elastic bodies)

Wave propagation

Stress and strain

DYNAMIC STRESS CONCENTRATION FACTORS

Technical Report WAL TR 811.6/1

by

Richard Shea

Date of Issue - March 1963

AMS Code 5011.11.838
Basic Research in Physical Sciences

D/A Project 1-A-0-10501-B-010

WATERTOWN ARSENAL
WATERTOWN 72, MASS.

WATERTOWN ARSENAL LABORATORIES

TITLE

DYNAMIC STRESS CONCENTRATION FACTORS

ABSTRACT

The problem of the response of structural discontinuities to short duration stress pulses is studied experimentally. Employing explosively induced stress pulses in thin plastic plates containing central circular holes, a dynamic stress concentration factor is determined as a function of pulse frequency. It is concluded for this loading case that the dynamic stress concentration is significantly lower than the static value.

Richard Shea

RICHARD SHEA
Mechanical Engineer

APPROVED:

J. F. Sullivan

J. F. SULLIVAN
Director
Watertown Arsenal Laboratories

CONTENTS

NOMENCLATURE

Symbol		Description
c_1	=	Dilatational wave velocity
c_2	=	Distortional wave velocity
d	=	Representative discontinuity dimension (hole diameter in this case)
E	=	Young's modulus
h	=	Thickness of shear plate
k	=	Stress concentration factor
t	=	Time
v	=	"Primacord" burning rate
v_o	=	Impact velocity of shear plate
w	=	Width of model
α	=	Angle of biased edge of model
ϵ_{max}	=	Maximum (peak pulse) strain
ϵ_{nom}	=	Nominal (peak pulse) strain
$\bar{\epsilon}_{nom}$	=	Nominal (peak pulse) strain corrected for attenuation
λ	=	Wave length of dilatational pulse
ν	=	Poisson's ratio
ρ	=	Mass density
σ_{max}	=	Maximum (peak pulse) stress
σ_{nom}	=	Nominal (peak pulse) stress
τ	=	Period of dilatational pulse

INTRODUCTION

Many studies have been made of stress distributions in the vicinity of discontinuities such as holes and notches. These studies, both theoretical and experimental, have provided a great deal of information on the behavior of many of the more common discontinuities under static loading. The usual design procedure for obtaining the maximum stresses associated with such discontinuities has been primarily a matter of applying the pertinent stress concentration factors to the nominal stresses obtained from the simple strength of materials formulae.

This design method has been generally adequate, and even conservative in many instances, for static loading considerations. When dynamic loads are involved, the usual recourse has been to follow the same procedure but to increase the margin of safety to allow for the uncertainty of the actual dynamic stress. Obviously, this approach will lead to an efficient design only by pure chance.

The purpose of this study then is to investigate some of the more general aspects of the behavior of discontinuities under dynamic loads. Specifically, the geometry considered here is a thin plate containing a central circular hole; and the loading is of a short duration, discrete pulse nature. The problem is approached experimentally using explosively induced stress pulses in thin plastic plates.

Single, discrete, compression pulses are propagated longitudinally through plates containing the discontinuities. The emphasis is directed toward stress pulses having durations that are much shorter than the fundamental dilatational period of the plates.

Some previous experimental work in this area has been undertaken by Durelli, et al.[1,2] Employing dynamic photoelastic techniques the same problem was investigated. In these studies, the pulse durations were several times longer than the period of the plates and, accordingly, no apparent dynamic effect was noted.

In the early phases of this program an attempt was made to generate short duration stress pulses by the use of a spring-propelled shear plate impacting the edge of a rectangular plate containing a central circular hole (see Figure 1). The alignment in this scheme was a highly critical factor, and the pulse lengths obtained were about five times the diameter of the holes. Again, the stress concentration factor observed was essentially equal to the static value.

Pao[3] has studied the problem of the vibratory loading of an infinite plate containing a central circular hole. In this theoretical approach it is noted that, when the wavelength of the vibration is of the same order of magnitude as the diameter of the hole, the maximum stress at the hole varies with the forcing frequency.

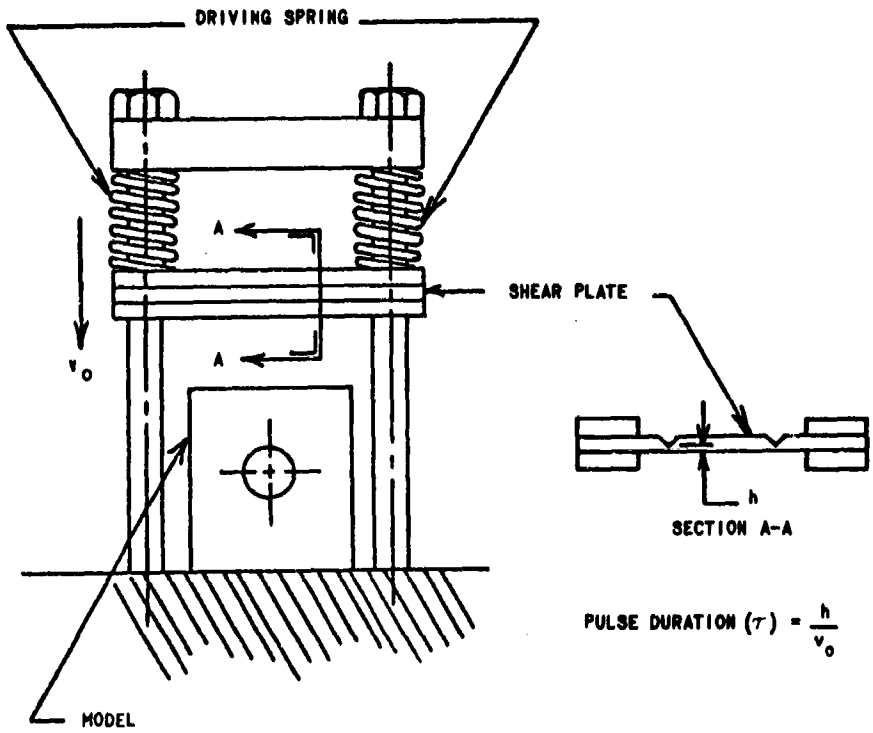

Figure 1. SCHEMATIC OF SPRING-PROPELLED LOADING DEVICE

FORMULATION

Dynamic Stress Concentration Factor

In the usual terminology for the case of plane stress, the stress concentration factor is expressed as the ratio of maximum to nominal stresses.*

$$k = \frac{\sigma_{max}}{\sigma_{nom}} \tag{1}$$

While this is based on static reasoning, it may be extended to include dynamic considerations with no loss of generality. Assuming the attenuation of the pulse to be insignificant, if σ_{nom} is defined as the peak pulse stress several wavelengths upstream of the discontinuity, and σ_{max} is defined as the peak pulse stress at the discontinuity, k will still portray the effect of the discontinuity.

* σ_{nom} is based on the net area at the discontinuity in both the static and dynamic sense, i.e., the effect of the absence of the material at the discontinuity is considered, but the associated nonuniform stress distribution is not.

The configurations considered here are such that at the points where both σ_{nom} and σ_{max} occur, a state of unixial stress exists. In the nominal stress field, during the time of initial pulse passage, there is no stress perpendicular to the direction of the pulse propagation. At the edge of the hole there can be no radial stress, so that there is a uniaxial stress in the tangential direction.

Therefore, the stress concentration factor can be written in terms of the nominal and maximum strains.

$$k = \frac{\epsilon_{max}}{\epsilon_{nom}} . \qquad (2)$$

Here the same restrictions regarding the definitions of the dynamic maximum and nominal stresses must be observed.

Pulse Frequency Parameter

Since an effect of pulse duration, or conversely pulse frequency, on the response at a discontinuity is suggested, a dependency is implied of the form:

$$k = f\left(\frac{d}{\lambda}\right) . \qquad (3)$$

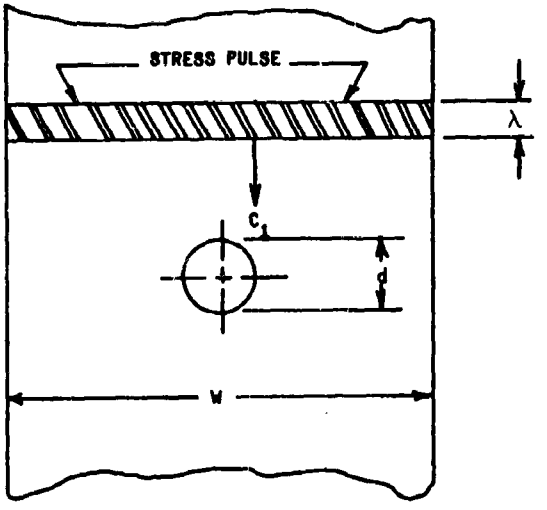

Figure 2. PROPAGATION OF STRESS PULSE IN FINITE PLATE CONTAINING CENTRAL CIRCULAR HOLE

Here d is a representative geometric dimension of the discontinuity, the hole diameter, in this case; and λ is the wavelength of the stress pulse. Figure 2 illustrates these dimensions for a plane compression pulse propagating longitudinally along a plate with a central circular hole.

The pulse wavelength is a function of both the material of the member and the duration of the applied load.

$$\lambda = c_1 \tau . \qquad (4)$$

The dilatational wave velocity (which is dependent solely on the material) is represented by c_1, and the loading duration by τ.

This study has been restricted to the effect of the dilatational (compression) pulse. Since there is also a distortional (shear) pulse associated with dynamic loading, attention must be directed to that portion of the member which is unaffected by the shear pulse (at least during the passage of the initial compression pulse). This is accomplished by observing only the initial response of the member at locations relatively far removed from the area at which the load is applied. In effect, the dilatational pulse is allowed sufficient room to "outrun" the distortional pulse. Inspection of Equations 5, below, will show that the dilatational velocity (c_1) is always greater than the distortional velocity (c_2).

$$c_1 = \sqrt{\frac{E}{\rho(1-\nu^2)}}$$

$$c_2 = \sqrt{\frac{E}{2\rho(1+\nu)}} \qquad (5)$$

EXPERIMENTAL TECHNIQUE

Models

Effort was directed toward obtaining pulse frequency parameters varying from about 1.0 to 5.0. However, since it is impractical to vary the pulse length, the variation of the $\frac{d}{\lambda}$ parameter was accomplished by changing the physical dimension, d. The significant geometric parameters were kept constant by scaling other pertinent model dimensions in the same proportion as d.

The models were fabricated from thin (1/4-inch Plexiglas) plastic plates. The use of plastic is desirable from several precepts. First, the elastic wave velocities in plastics are considerably lower than in most metals. Thus, it is possible to achieve desirable (i.e., relatively large) $\frac{d}{\lambda}$ values without having to resort to large and, therefore, unwieldy models. Second, plastics possess low elastic moduli so that small loads will produce strains sufficiently large for accurate measurement.

The plates were generally in the form of trapezoids. The over-all dimensions varied from about 4" x 10" to 36" x 60" in order to bracket a sufficient range of the pulse frequency parameter. The discontinuities considered in the initial phase of this study were central circular holes varying from 1.0 to 9.0 inch diameters.

Loading

Lengths of Primacord detonating fuse were placed along the biased edge of the models as shown in Figure 3. Detonation of the fuse was accomplished by initiation of a No. 6 blasting cap at the upper end of the Primacord. The burning rate of the Primacord is approximately 250,000 inches per second; and the burning duration, at a point, about 20 microseconds.

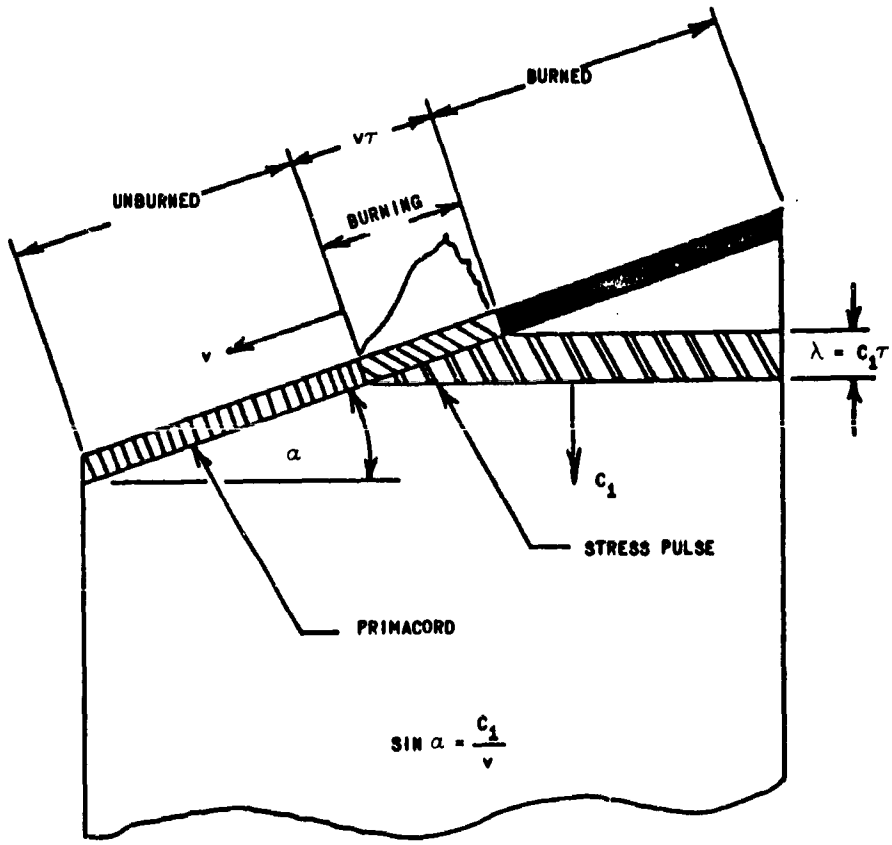

Figure 3. LOADING TECHNIQUE

This technique, which is attributed to Christie,[4] imparts sharp, reproducible pulses, of about 20 microseconds duration, to the plate. Referring again to Figure 3, if the angle α, between the bias and the horizontal, is set such that $\sin \alpha = \frac{c_1}{v}$ (where v is the burning rate of the Primacord), it is possible to obtain a short duration pulse which propagates longitudinally down the model.

Some initial experimentation was necessary to determine the correct value of α.* This was due to the variability of Young's modulus with strain rate which, in turn, affects the wave velocities. Essentially, the velocity of the dilatational wave was determined by measuring the time delay of its arrival at two points on a longitudinal line; and the angle, α, adjusted accordingly. To check the angle, the arrival of the pulse at two points on the same transverse line, but at opposite edges of the plate, was noted.

The pulses generated by this method were quite reproducible, having durations of 20 microseconds, which in Plexiglas correspond to a wavelength of 1.9 inches. Although the amplitudes of pulses on different models were not identical (due probably to the variation of the explosive loading in the Primacord), the method faithfully reproduced pulses of the same duration and general shape. Figure 4 is a tracing of a typical oscilloscope record showing the pulse shape obtained by this loading technique.

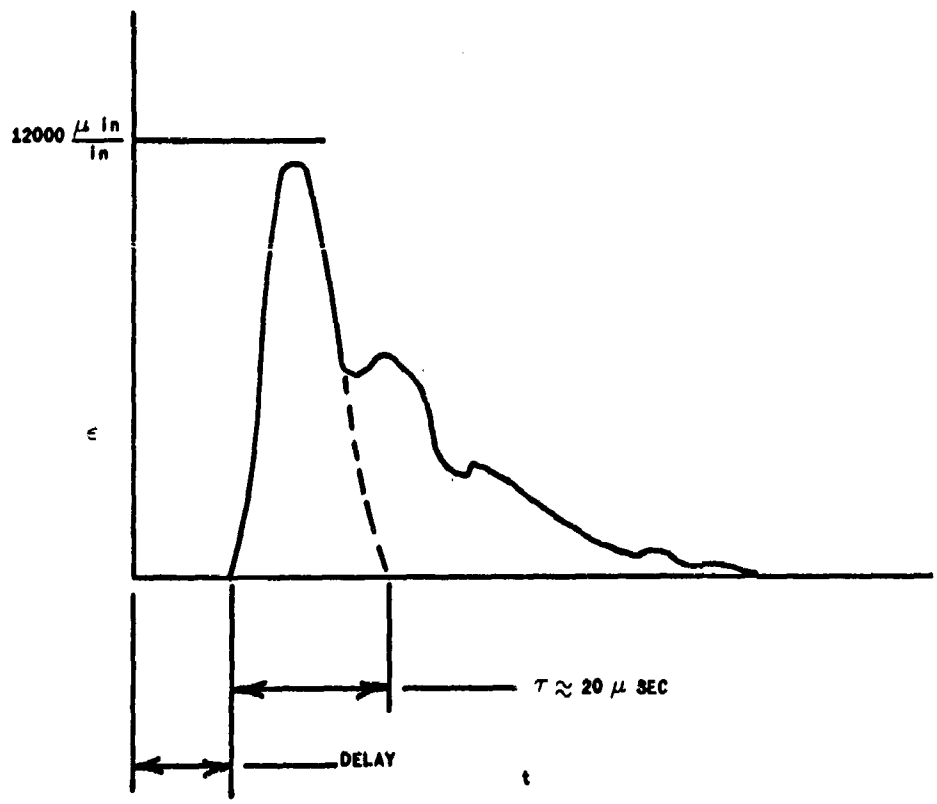

Figure 4. TYPICAL STRAIN PULSE

*For Plexiglas, α is approximately 25 degrees. If steel or aluminum were employed as the model material, α would have to be about 75 degrees, which would have been quite awkward. This, then, is another reason for employing a plastic model.

Instrumentation

The instrumentation employed in this study consisted of 1/16-inch foil strain gages, a trigger gage, suitable ballast circuits, and dual beam oscilloscopes. This is shown schematically in Figure 5.

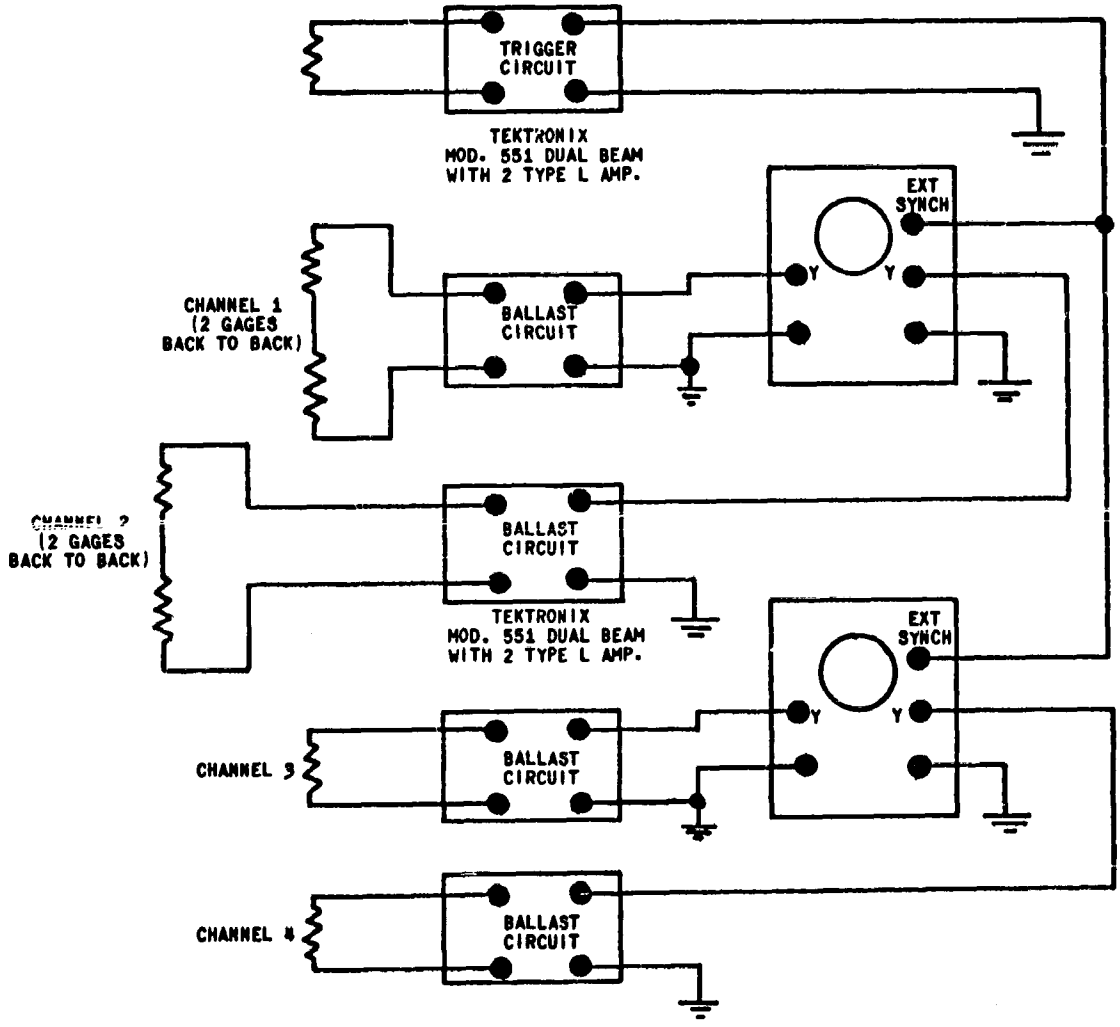

Figure 5. SCHEMATIC OF STRAIN GAGE CIRCUIT

The oscilloscopes were triggered by the strain signal from a gage in the nominal stress field. This signal was delayed sufficiently to insure observance of the entire strain phenomenon. The delay may be seen in Figure 4 at the origin of the trace.

The strain gages were located typically as shown in Figure 6. Four gages were mounted in the nominal stress field (at two locations on the surface of the model, and back-to-back). The back-to-back gages were employed to cancel the effect of pulse variations through the thickness of the model.* The two locations on the same horizontal line of the plate provided assurance of pulse orientation and amplitude across the model. The nominal strain was obtained by averaging the outputs of the two gage pairs. In all cases the times of pulse arrival at the two transverse locations were generally coincident within 1 or 2 microseconds.

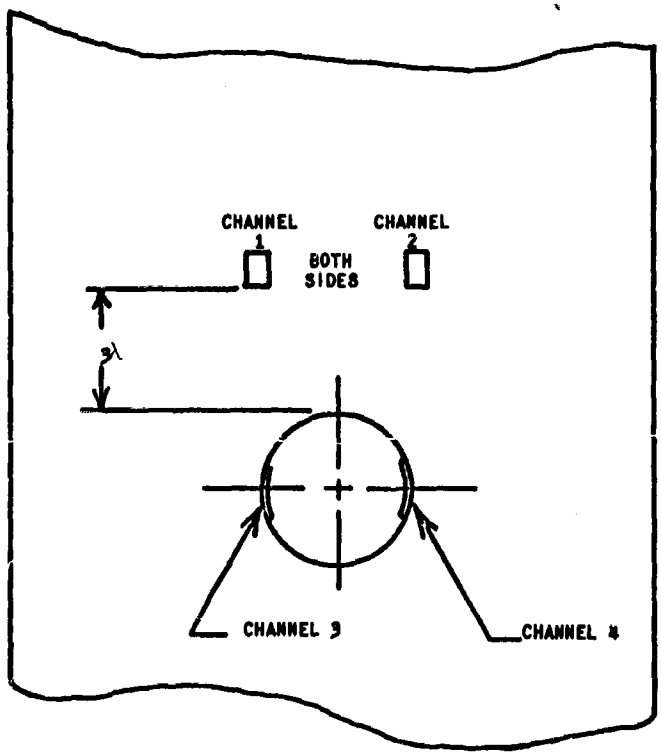

CHANNELS 1 & 2 - NOMINAL STRAIN
CHANNELS 3 & 4 - MAXIMUM STRAIN

Figure 6. LOCATION OF STRAIN GAGES

Also as shown in Figure 6, two gages were located at the opposite transverse extremities of the hole. Again, this was done to provide assurance of pulse uniformity. The orientation of the pulse passage at this location was essentially horizontal within several microseconds in all cases.

*No strain differences through the thickness were noted, however. The back gages could be properly omitted with no loss of accuracy.

Limitations

Response of Strain Gages on Plastics

Clark[5] has noted that wire resistance strain gages mounted on 1/2-inch-square bars of CR-39 plastic exhibited only about 75% of the strain sensitivity that would be expected. The effect was noted both statically and dynamically in relatively close agreement and was attributed to the wire of the strain gages stiffening the plastic.

Assuming that this reduction in sensitivity is constant, the stress concentration factor, being simply a ratio of strains, should be unaffected. However, since the stiffness of the models at the regions of nominal and maximum stress differs significantly (at least in the static sense), it was decided to observe this phenomenon for the particular configuration being studied.

A sheet of HYSOL 6000 OP, a birefringent plastic having physical properties similar to Plexiglas, was fabricated into a model with the same geometric parameters as the models used in the primary testing phase. The model was loaded statically in tension and the maximum and nominal stresses determined photoelastically. After unloading, foil strain gages were applied as on the dynamic models. The model was loaded again and the maximum and nominal stresses determined, this time from the output of the strain gages.

The comparison between these data indicated that the foil strain gages gave results for both the nominal and maximum strains which were as close to the photoelastic values as could be reasonably expected.

The fact that the reduced strain sensitivity did not occur in this study may be due to the use of foil-type strain gages which are not as stiff as wire gages. In any event, since the static check showed no significant loss of strain sensitivity, it is felt that, dynamically, any error which may exist may be properly neglected.

Dynamic Response of Strain Gages

There is some tendency to doubt the validity of strain gage response to high frequency excitation. For example, while studying the propagation of plastic waves in soft aluminum, Gillich[6] noted that resistance strain gage measurements deviated significantly from diffraction grating readings at strains above 2%, and at strain rates corresponding to wave velocities. However, in the present study, the maximum strains recorded were always much lower than 2%, generally in the range of 12,000 to 15,000 microinches per inch.

On the other hand, while Clark[5] did find a difference in dynamic strains between strain gage measurements and photoelastic techniques, the identical difference was observed statically.

One prevalent criticism of employing strain gages for high frequency measurements stems from a lack of confidence in the dynamic qualities of adhesives. While this is, no doubt, an area worthy of additional investigation, it was found in this study that the adhesive bond was generally excellent and, in practically all cases, the gages were found to be securely bonded after the test.

Attenuation of the Stress Pulse

One of the assumptions made in the formulation of the equations for the dynamic stress concentration factor was that the attenuation of the pulse between the locations of the nominal and maximum stresses could be neglected. However, the attenuation is actually significant, and it was therefore necessary to apply correction factors to account for the pulse decay.

A series of tests was conducted on models with no discontinuities, but otherwise identical to the models used in the primary testing phase. A correction factor was determined for each of the model sizes and applied to the nominal strains. The corrected nominal strains were then employed in the determination of the stress concentrations.

Using this concept, Equation 3 may be rewritten:

$$k = \frac{\epsilon_{max}}{\bar{\epsilon}_{nom}} \qquad (6)$$

where $\bar{\epsilon}_{nom}$ is the attenuated nominal strain.

RESULTS AND CONCLUSIONS

The results of this study are indicated in Figure 7*. As may be noted, there is a pronounced variation of the stress concentration factor with pulse frequency, particularly in the region of pulses of the same length as the hole diameter, where it drops off significantly.

This may be explained by a purely physical argument of the stress pulse propagation. Since the band of stressed material is about the same length as the discontinuity, there is not sufficient time or space for a secondary pulse to be reflected from the hole boundary and reinforce the main pulse.

*Pao's results for an infinite plate with a circular hole under vibratory loading (Figure 3, Reference 3) are superposed on this figure. While the cases examined are somewhat different, the agreement in the trend is significant.

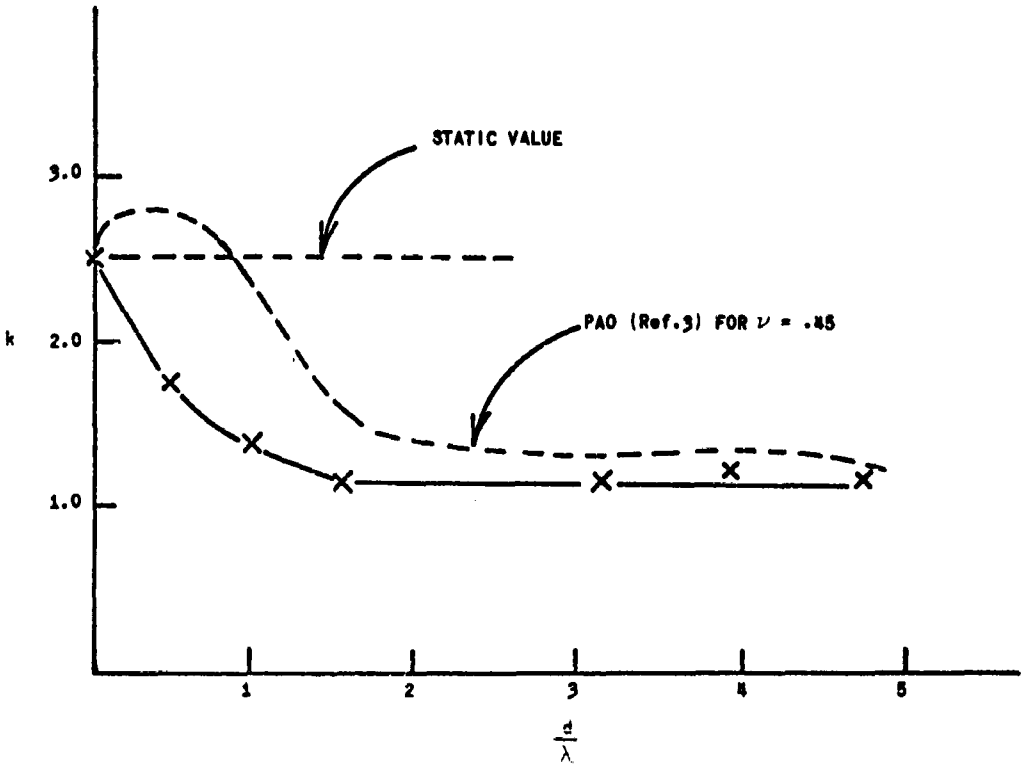

Figure 7. VARIATION OF STRESS CONCENTRATION WITH PULSE FREQUENCY

As the band is diminished relatively to the whole, there is even less opportunity for reinforcement to occur. On the other hand, for long duration pulses the band becomes quite large (approaching a static loading condition) and there is sufficient reinforcement to bring about a high stress concentration factor.

It may be concluded from this study that static criteria are not necessarily valid in the dynamic sense. For the particular case considered, the results applied to a design problem would be striking because not only would the designer use a conservative static stress concentration factor, but he would probably compound the inefficiency by resorting to a heavy margin of safety.

ACKNOWLEDGMENT

The author wishes to acknowledge Messrs. Joseph I. Bluhm and John J. Hannon of the U. S. Army Materials Research Agency: to Mr. Bluhm for suggesting the problem, and for his advice and encouragement; to Mr. Hannon for designing and setting up the instrumentation, directing the experimental program, and assisting in many ways too numerous to elucidate.

REFERENCES

1. DURELLI, A. J., DALLY, J. W., and RILEY, W.F., Stress Concentration Factors Under Dynamic Loading Conditions, Armour Research Foundation, AFOSR-TN-58-892, 1958.

2. DURELLI, A. J., and RILEY, W.F., Stress Distribution on the Boundary of a Circular Hole in a Large Plate During Passage of a Stress Pulse of Long Duration, ASME Paper No. 61-APM-4, 1961.

3. YIH-HSING PAO, Dynamical Stress Concentration in an Elastic Plate, ASME Paper No. 61-APMW-17, 1961.

4. CHRISTIE, D. G., Reflection of Elastic Waves from a Free Boundary, Philosophical Magazine, v. 46, 1955, p. 527-541.

5. CLARK, A. B. J., Static and Dynamic Calibration of a Photoelastic Model Material, CR-39, SESA Proceedings, v. XIV, no. 1, 1957.

6. GILLICH, W. J., The Response of Bonded Wire Resistance Strain Gages to Large Amplitude Waves in Annealed Aluminum, Master's Essay, The Johns Hopkins University, 1960.

WATERTOWN ARSENAL
WATERTOWN 72, MASSACHUSETTS

TECHNICAL REPORT DISTRIBUTION

Report No.: WAL TR 811.6/1 March 1963 Title: Dynamic Stress Concentration Factors

Distribution List approved by 1st Indorsement from Ordnance Weapons Command, ORDOW-TB, dated 4 January 1962

No. of Copies	TO
	Office of the Director of Defense Research and Engineering, Room 3D-1067, The Pentagon, Washington 25, D. C.
1	ATTN: Mr. J. C. Barrett
	Commander, Armed Services Technical Information Agency, Arlington Hall Station, Arlington 12, Virginia
10	ATTN: TIPDR
	Advanced Research Project Agency, The Pentagon, Washington 25, D.C.
1	ATTN: Dr. G. Mock
1	Solid Propellant Information Agency, Applied Physics Laboratory, The Johns Hopkins University, Silver Spring, Maryland
	Commanding General, U. S. Army Materiel Command, Washington 25, D.C.
1	ATTN: AMCRD-RS
	Commanding General, U. S. Army Missile Command, Redstone Arsenal, Alabama
2	ATTN: AMSMI-RB, Redstone Scientific Information Center
1	AMSMI-RRS, Mr. R. E. Ely
1	AMSMI-RKX, Mr. R. Fink
1	AMSMI, Mr. W. K. Thomas
1	AMSMI-RSM, Mr. E. J. Wheelahan
1	Commanding General, U. S. Army Mobility Command, Detroit 9, Michigan
1	Commanding General, U. S. Army Munitions Command, Dover, New Jersey
	Commanding General, U. S. Army Test and Evaluation Command, Aberdeen Proving Ground, Maryland
2	ATTN: AMSTE, Technical Library
	Commanding General, U. S. Army Weapons Command, Rock Island, Illinois
1	ATTN: AMSWE-IX, Industrial Division
1	AMSWE-TX, Research Division
1	AMSWE-IM, Industrial Mobilization Branch
1	AMSWE-GU, Security Officer

No. of Copies	TO
	Commanding Officer, Harry Diamond Laboratories, Connecticut Avenue and Van Ness Street, N. W., Washington 25, D.C.
1	ATTN: AMXDO-TIB
	Commanding Officer, Frankford Arsenal, Philadelphia 37, Pennsylvania
1	ATTN: ORDBA-1330
1	ORDBA-0270, Library
	Commanding Officer, Picatinny Arsenal, Dover, New Jersey
1	ATTN: AMSMU, Mr. J. J. Scavuzzo, Plastics and Packaging Laboratory
1	Commanding Officer, PLASTEC, Picatinny Arsenal, Dover, New Jersey
	Commanding Officer, Springfield Armory, Springfield 1, Massachusetts
1	ATTN: SWESP-TX, Research and Development Division
	Commanding Officer, Watertown Arsenal, Watertown 72, Massachusetts
1	ATTN: SMIWT-EX, Chief, Engineering Division
1	SMIWT-OE, Industrial Engineering Section
	Commanding Officer, Watervliet Arsenal, Watervliet, New York
1	ATTN: SWEWV-RR
	Commanding General, U. S. Army Chemical Warfare Laboratories, Army Chemical Center, Maryland
1	ATTN: Technical Library
1	Commanding Officer, U. S. Army Environmental Health Laboratory, Army Chemical Center, Maryland
	Commanding Officer, Engineering Research and Development Laboratory, Fort Belvoir, Virginia
1	ATTN: Materials Branch
	Commanding General, Quartermaster Research and Development Command, Natick, Massachusetts
1	ATTN: AMXRC, Clothing and Organic Materials Division
	Headquarters, U. S. Army Signal Research and Development Laboratory, Fort Monroe, Virginia
1	ATTN: Materials Branch
1	Director, Army Research Office, Office, Chief of Research and Development, U. S. Army, The Pentagon, Washington 25, D. C.
1	Commanding Officer, U. S. Army Research Office (Durham), Box CM, Duke Station, Durham, North Carolina

No. of Copies	TO
	Chief of Research and Development, U. S. Army Research and Development Liaison Group, APO 757, New York
1	ATTN: Dr. B. Stein
	Chief, Bureau of Naval Weapons, Department of the Navy, Room 2225, Munitions Building, Washington 25, D. C.
1	ATTN: RMMP
	Chief, Bureau of Ships, Department of the Navy, Washington 25, D.C.
1	ATTN: Code 344
	Chief, Office of Naval Research, Department of the Navy, Washington 25, D. C.
1	ATTN: Code 423
	Chief, Special Projects Office, Bureau of Naval Weapons, Department of the Navy, Washington 25, D. C.
1	ATTN: SP 271
	Commander, U. S. Naval Ordnance Laboratory, White Oak, Silver Spring, Maryland
1	ATTN: WM
	Commander, U. S. Naval Ordnance Test Station, China Lake, California
1	ATTN: Technical Library Branch
	Commander, U. S. Naval Research Laboratory, Anacostia Station, Washington 25, D. C.
1	ATTN: Technical Information Center
	U. S. Air Force Directorate of Research and Development, Room 4D-313, The Pentagon, Washington 25, D. C.
1	ATTN: Lt. Col. J. B. Shipp, Jr.
	ARDC Flight Test Center, Edwards Air Force Base, California
1	ATTN: Solid Systems Division, FTRSC
	AMC Aeronautical Systems Center, Wright-Patterson Air Force Base, Ohio
2	ATTN: Manufacturing and Materials Technology Division, LMBMO
	National Aeronautics and Space Administration, 1520 H Street, N.W., Washington 25, D. C.
1	ATTN: Mr. G. C. Deutsch
1	Mr. R. V. Rhode

No. of Copies	TO
	Jet Propulsion Laboratory, California Institute, 4800 Oak Grove Drive, Pasadena, California
1	ATTN: Dr. L. Jaffe
	George C. Marshall Space Flight Center, National Aeronautics and Space Flight Administration, Huntsville, Alabama
1	ATTN: M-S&M-M
1	M-F&AE-M
	Commanding Officer, U. S. Army Materials Research Agency, Watertown 72, Massachusetts
5	ATTN: AMXMR-LXM, Technical Information Section
1	AMXMR-OPT
1	AMXMR, Dr. R. Beeuwkes, Jr.
1	Author

69 -- TOTAL COPIES DISTRIBUTED

AD _____ Accession No. _____

Watertown Arsenal Laboratories, Watertown 72, Mass.
DYNAMIC STRESS CONCENTRATION FACTORS - Richard Shea

Report No. WAL TR 811.6/1, March 1963, 14 pp - illus, AMS Code 5011.11.838, D/A Proj 1-A-0-10501-B-010, Unclassified Report

The problem of the response of structural discontinuities to short duration stress pulses is studied experimentally. Employing explosively induced stress pulses in thin plastic plates containing central circular holes, a dynamic stress concentration factor is determined as a function of pulse frequency. It is concluded for this loading case that the dynamic stress concentration is significantly lower than the static value.

NO DISTRIBUTION LIMITATIONS

UNCLASSIFIED

1. Dynamics (elastic bodies)
2. Wave propagation
3. Stress and strain

I. Shea, Richard

II. AMS Code 5011.11.838

III. D/A Project 1-A-0-10501-B-010

AD _____ Accession No. _____

Watertown Arsenal Laboratories, Watertown 72, Mass.
DYNAMIC STRESS CONCENTRATION FACTORS - Richard Shea

Report No. WAL TR 811.6/1, March 1963, 14 pp - illus, AMS Code 5011.11.838, D/A Proj 1-A-0-10501-B-010, Unclassified Report

The problem of the response of structural discontinuities to short duration stress pulses is studied experimentally. Employing explosively induced stress pulses in thin plastic plates containing central circular holes, a dynamic stress concentration factor is determined as a function of pulse frequency. It is concluded for this loading case that the dynamic stress concentration is significantly lower than the static value.

NO DISTRIBUTION LIMITATIONS

UNCLASSIFIED

1. Dynamics (elastic bodies)
2. Wave propagation
3. Stress and strain

I. Shea, Richard

II. AMS Code 5011.11.838

III. D/A Project 1-A-0-10501-B-010

AD _____ Accession No. _____

Watertown Arsenal Laboratories, Watertown 72, Mass.
DYNAMIC STRESS CONCENTRATION FACTORS - Richard Shea

Report No. WAL TR 811.6/1, March 1963, 14 pp - illus, AMS Code 5011.11.838, D/A Proj 1-A-0-10501-B-010, Unclassified Report

The problem of the response of structural discontinuities to short duration stress pulses is studied experimentally. Employing explosively induced stress pulses in thin plastic plates containing central circular holes, a dynamic stress concentration factor is determined as a function of pulse frequency. It is concluded for this loading case that the dynamic stress concentration is significantly lower than the static value.

NO DISTRIBUTION LIMITATIONS

UNCLASSIFIED

1. Dynamics (elastic bodies)
2. Wave propagation
3. Stress and strain

I. Shea, Richard

II. AMS Code 5011.11.838

III. D/A Project 1-A-0-10501-B-010

AD _____ Accession No. _____

Watertown Arsenal Laboratories, Watertown 72, Mass.
DYNAMIC STRESS CONCENTRATION FACTORS - Richard Shea

Report No. WAL TR 811.6/1, March 1963, 14 pp - illus, AMS Code 5011.11.838, D/A Proj 1-A-0-10501-B-010, Unclassified Report

The problem of the response of structural discontinuities to short duration stress pulses is studied experimentally. Employing explosively induced stress pulses in thin plastic plates containing central circular holes, a dynamic stress concentration factor is determined as a function of pulse frequency. It is concluded for this loading case that the dynamic stress concentration is significantly lower than the static value.

NO DISTRIBUTION LIMITATIONS

UNCLASSIFIED

1. Dynamics (elastic bodies)
2. Wave propagation
3. Stress and strain

I. Shea, Richard

II. AMS Code 5011.11.838

III. D/A Project 1-A-0-10501-B-010